

Synthesis, structure, and magnetism of three manganese-organic framework with PtS topology

MENG QingGuo^{1,2}, DAI FangNa^{3*}, ZHANG LiangLiang³,
WANG RongMing³ & SUN DaoFeng^{1,3*}

¹Key Lab of Colloid and Interface Chemistry, Ministry of Education; School of Chemistry and Chemical Engineering, Shandong University, Jinan 250100, China

²Chemistry & Chemical and Environmental Engineering College, Weifang University, Weifang 261061, China

³College of Science, China University of Petroleum (East China), Qingdao 266580, China

Received January 13, 2014; accepted April 1, 2014; published online September 18, 2014

Three 3D manganese-organic frameworks, $\text{Mn}_2(\text{BPTC})(\text{DMF})_2(\text{H}_2\text{O}) \cdot \text{DMF} \cdot 3\text{H}_2\text{O}$ (**1**), $\text{Mn}_2(\text{BPTC})(\text{bipy})(\text{DMF}) \cdot \text{DMF} \cdot \text{H}_2\text{O}$ (**2**), and $\text{Mn}_2(\text{BPTC})(\text{phen})(\text{DMF}) \cdot \text{EtOH}$ (**3**), have been solvothermally synthesized using 3,3',5,5'-biphenyltetracarboxylic acid (H₄BPTC). All complexes are characterized by PXRD, EA, IR and TG. The results show that they all bear the PtS topology with (4².8⁴) (4².8⁴) for the vertex symbols of the planar and tetrahedral nodes, in which the BPTC ligand is considered as a square-planar 4-connected linker, and every binuclear SBU connected to the four BPTC ligands is simplified into tetrahedral 4-connected nodes. Because the three coordination sites of one metal center of SBU are occupied by the coordinated solvent molecules, complex **1** exhibits low stability. After substituting 2,2'-bipy or 1,10-phen for two coordinated solvent molecules, complexes **2** and **3** display evidently higher structure stability. The magnetism property of complex **2** is also discussed in detail.

metal-organic frameworks, manganese, PtS topology, solvothermal synthesis, magnetism

1 Introduction

Design and synthesis of metal-organic frameworks (MOFs) with desired topologies and properties are an attractive field in supramolecular chemistry and crystal engineering because of their potential applications in a variety of areas, including catalysis, ion exchange, sensors, shape-selective adsorption, gas storage, photochemistry, and materials with magnetic properties [1–15]. MOFs are new type of hybrid materials made from various metal ions and organic ligands [16–20]. Thus, the coordination geometries of metal ions and the conformations of organic ligands have significant influence on the final structure of the products [21–26]. In the past decades, many MOFs bearing interesting topologies

and properties have been designed and synthesized based on various metal ions such as Cu²⁺, Zn²⁺, Co²⁺, Mn²⁺, and carboxylate ligands, such as terephthalic acid and benzenetricarboxylic acid [27–37].

Because carboxylate ligands possess strong coordination abilities and different coordination modes, they can link the metal ions to generate various topological structures with 1D, 2D, and 3D frameworks [38–40]. Much efforts have been devoted to the construction of three-dimensional porous MOFs based on multi-carboxylate ligands [41, 42]. Among MOFs with known topologies, PtS nets have been widely documented as this kind of topological MOFs can be easily obtained through a tetrahedral linker and a square-planar node [43]. Indeed, many porous MOFs with PtS topologies were synthesized and characterized based on the tetrahedral ligands and square-planar SBUs in the past decades [44–46]. However, MOFs with PtS topology based

*Corresponding authors (email: fndai@upc.edu.cn; dfsun@sdu.edu.cn)

on the square-planar organic linkers and tetrahedral SBUs are rare [47–53].

In this work, three 3D manganese-organic frameworks, $\text{Mn}_2(\text{BPTC})(\text{DMF})_2(\text{H}_2\text{O}) \cdot \text{DMF} \cdot 3\text{H}_2\text{O}$ ($\text{DMF} = N,N$ -dimethylformamide) (**1**), $\text{Mn}_2(\text{BPTC})(\text{bipy}) \cdot \text{DMF} \cdot \text{H}_2\text{O}$ (**2**), and $\text{Mn}_2(\text{BPTC})(\text{phen})(\text{DMF}) \cdot \text{EtOH}$ (**3**), were synthesized using $\text{Mn}(\text{NO}_3)_2$ and 3,3',5,5'-biphenyltetracarboxylic acid (H_4BPTC , Scheme 1). Single-crystal X-ray diffraction reveals that the square-planar ligands link the binuclear metal centers to generate PtS topology for all the three structures. Meanwhile, the binuclear SBU is engaged by four carboxylate groups from four different BPTC ligands. In compounds **1–3**, the remaining coordination sites of the SBU were occupied by coordinated solvent molecules, and chelating ligands 2,2'-bipyridine (bipy) and 1,10-phenanthroline (phen), respectively.

2 Experimental

2.1 General experimental information

All of the chemicals and solvents used in the syntheses were of analytical grade and used without further purification. C, N, and H analyses were performed on an EA1110 CHNS-O CE 65 elemental analyzer (CE Instruments, Italy). IR (KBr pellet) spectra were recorded on a Nicolet Magna 750FT-IR spectrometer (USA). Thermogravimetric analyses (TGA) were performed on a Netzsch STA 449C thermal analyzer (Germany) from room temperature to 700 °C under nitrogen atmosphere at a heating rate of 10 °C/min.

2.2 Crystal structure determinations

Crystallographic data for **1–3** were collected on a Bruker Smart APEXII CCD diffractometer (Germany) with Mo K α ($\lambda = 0.71073 \text{ \AA}$) at room temperature. All the structures were solved by the direct method using the SHELXS program of the SHELXTL package and refined by the full-matrix least-squares method using SHELXL [54, 55]. The metal atoms in each complex were located from the E-maps, and other non-hydrogen atoms were located in successive difference Fourier syntheses and refined using anisotropic thermal parameters on F^2 . The organic hydrogen

atoms were generated geometrically (C–H 0.96 Å). The crystallographic data (excluding structure factors) for the structures reported in this paper have been deposited in the Cambridge Crystallographic Data Center with CCDC Numbers: 969316–969318. Crystallographic data for **1–3** are summarized in Table 1 and the selected bond lengths and bond angles are listed in Table S1 (Supporting Information online).

2.3 Synthesis of $\text{Mn}_2(\text{BPTC})(\text{DMF})_2(\text{H}_2\text{O}) \cdot \text{DMF} \cdot 3\text{H}_2\text{O}$ (**1**)

A mixture of $\text{Mn}(\text{NO}_3)_2$ (0.05 mL, 50% aq.), H_4BPTC (1 mg, 0.003 mmol), NaOH (0.05 mL, 0.5 mol/L), and DMF– $\text{C}_2\text{H}_5\text{OH}$ – H_2O (1 mL, 2:1:1) were sealed in a pressure-resistant glass tube and put into a programmed oven, slowly heated to 75 °C at room temperature in 400 min, and kept at 75 °C for 4320 min. After slowly cooling to 30 °C in 800 min, colorless block crystals of **1** were separated in 35.3% yield based on H_4BPTC . Elemental analysis calcd. (%) for **1**: C 41.28, H 4.82, N 5.78; found (%): C 41.21, H 4.75, N 5.82%.

2.4 Synthesis of $\text{Mn}_2(\text{BPTC})(\text{bipy})(\text{DMF}) \cdot \text{DMF} \cdot \text{H}_2\text{O}$ (**2**)

A mixture of $\text{Mn}(\text{NO}_3)_2$ (0.05 mL, 50% aq.), H_4BPTC (1 mg, 0.003 mmol), 2,2'-bipy (3 mg, 0.019 mmol), NaOH (0.05 mL, 0.5 mol/L), and DMF– $\text{C}_2\text{H}_5\text{OH}$ – H_2O (1 mL, 2:1:1) were sealed in a pressure-resistant glass tube and put into a programmed oven, slowly heated to 75 °C at room temperature in 400 min, and kept at 75 °C for 4320 min. After slowly cooling to 30 °C in 800 min, colorless block crystals of **2** were separated in 38.2% yield based on H_4BPTC . Elemental analysis calcd. (%) for **2**: C 50.81, H 4.00, N 7.41; found (%): C 51.19, H 4.23, N 7.64%.

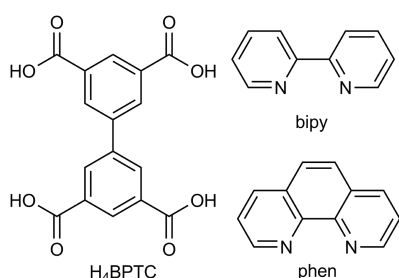
2.5 Synthesis of $\text{Mn}_2(\text{BPTC})(\text{phen})(\text{DMF}) \cdot \text{EtOH}$ (**3**)

A mixture of $\text{Mn}(\text{NO}_3)_2$ (0.05 mL, 50% aq.), H_4BPTC (1 mg, 0.003 mmol), phen (4 mg, 0.02 mmol), NaOH (0.05 mL, 0.5 mol/L), and DMF– $\text{C}_2\text{H}_5\text{OH}$ – H_2O (1 mL, 2:1:1) were sealed in a pressure-resistant glass tube and put into a programmed oven, slowly heated to 70 °C at room temperature in 600 min, and kept at 70 °C for 5000 min. After slowly cooling to 30 °C in 900 min, colorless block crystals of **3** were separated in 41% yield based on H_4BPTC . Elemental analysis calcd. (%) for **3**: C 50.81, H 4.00, N 7.41; found (%): C 51.19, H 4.23, N 7.64%.

3 Results and discussion

3.1 Structural description

Complexes **1–3** were synthesized through solvothermal



Scheme 1 Ligands involved in this work.

Table 1 Crystal data for **1–3**

	1	2	3
Empirical formula	C ₂₅ H ₂₉ Mn ₂ N ₃ O ₁₂	C ₃₂ H ₂₈ Mn ₂ N ₄ O ₁₀	C ₃₁ H ₁₈ Mn ₂ N ₃ O ₉
Formula weight	673.39	738.46	686.36
Crystal system	monoclinic	monoclinic	monoclinic
Space group	P2 ₁ /c	P2 ₁ /c	P2 ₁ /c
<i>a</i> (Å)	14.5460(5)	13.288(2)	13.153(3)
<i>b</i> (Å)	13.0153(4)	13.919(2)	13.986(4)
<i>c</i> (Å)	22.0633(8)	21.539(3)	21.683(4)
α (°)	90	90.00	90
β (°)	125.319(2)	121.502(7)	121.056(11)
γ (°)	90	90.00	90
Volume (Å ³)	3408.2(2)	3396.6(9)	3417.0(14)
<i>Z</i>	4	4	4
ρ_{calc} (mg/mm ³)	1.312	1.444	1.334
<i>F</i> (000)	1384.0	1512.0	1388.0
Crystal size (mm ³)	0.12 × 0.11 × 0.1	0.13 × 0.11 × 0.1	0.12 × 0.11 × 0.1
2θ range for data collection	3.446° to 49.998°	3.6° to 50°	3.646° to 49.998°
Index ranges	17 ≤ <i>h</i> ≤ 15, 15 ≤ <i>k</i> ≤ 15, 19 ≤ <i>l</i> ≤ 26	9 ≤ <i>h</i> ≤ 15, 16 ≤ <i>k</i> ≤ 16, 25 ≤ <i>l</i> ≤ 24	15 ≤ <i>h</i> ≤ 14, 16 ≤ <i>k</i> ≤ 12, 24 ≤ <i>l</i> ≤ 25
Reflections collected	16650	16237	16419
Independent reflections	6093 [<i>R</i> (int) = 0.0407]	5959 [<i>R</i> (int) = 0.0343]	6013 [<i>R</i> (int) = 0.0488]
Data/restraints/parameters	6093/222/385	5959/0/436	6013/24/407
Goodness-of-fit on <i>F</i> ²	1.076	1.138	1.044
Final <i>R</i> indexes [<i>I</i> ≥ 2σ(<i>I</i>)]	<i>R</i> ₁ = 0.0624, <i>wR</i> ₂ = 0.1799	<i>R</i> ₁ = 0.0505, <i>wR</i> ₂ = 0.1527	<i>R</i> ₁ = 0.0812, <i>wR</i> ₂ = 0.2449
Final <i>R</i> indexes [all data]	<i>R</i> ₁ = 0.0766, <i>wR</i> ₂ = 0.1912	<i>R</i> ₁ = 0.0679, <i>wR</i> ₂ = 0.1700	<i>R</i> ₁ = 0.1181, <i>wR</i> ₂ = 0.2829
Largest diff. peak/hole (e/Å ³)	1.36/-1.39	0.85/-0.78	1.42/-1.27

reactions based on H₄BPTC and manganese ions. The crystal structures were determined by single-crystal X-ray diffraction. The formula of Mn₂(BPTC)(DMF)₂(H₂O) · DMF · 3H₂O (**1**), Mn₂(BPTC)(bipy) (DMF) · DMF · H₂O (**2**), and Mn₂(BPTC)(phen)(DMF) · EtOH (**3**) were further confirmed by PXRD (Figure S1), elemental analysis, TGA, and IR (Figure S2). Complexes **1–3** are all three-dimensional frameworks based on binuclear manganese SBUs.

Complex **1** crystallizes in the monoclinic *P*2₁/c space. The asymmetric unit consists of two Mn²⁺ ions, one BPTC ligand, two coordinated DMF molecules, one coordinated water molecule, one uncoordinated DMF molecule and three uncoordinated molecules (Figure 1). In the crystal structure, there are two types of manganese ions with different coordination environments: Mn1 is coordinated by six oxygen atoms from four carboxylate groups in a distorted octahedral geometry, whereas Mn2 is coordinated by three oxygen atoms from three carboxylate groups, two coordinated DMF molecules, and one coordinated water molecule, in an octahedral geometry. The average Mn–O distance is 2.193 Å.

Mn1 and Mn2 are engaged by four carboxylate groups from four different ligands to generate a binuclear Mn SBU with the Mn–Mn distance being 3.495 Å. The remaining coordination sites of Mn1 are occupied by the coordinated DMF and water molecules, respectively. Thus, each binuclear

SBU attaches to four BPTC ligands and every ligand connects four binuclear SBUs to construct a three-dimensional framework. There exist 1D channels along the *c* axis, in which the coordinated DMF and uncoordinated DMF molecules reside (Figure 1). The approximate channel size for compound **1** is 9.1 × 9.3 Å. The percent void volume obtained using the PLATON software is 35.1% in the 3D network of **1**.

Topologically, each BPTC ligand connects four binuclear manganese SBUs; meanwhile, the BPTC ligand can be considered as a square-planar 4-connected linker, and every binuclear SBU, which is connected to the four BPTC ligands, can be simplified into tetrahedral 4-connected node. Based on the simplification, complex **1** possesses a 3D PtS topology with (4².8⁴) (4².8⁴) for the vertex symbols of the planar and tetrahedral nodes (Figure 2).

As mentioned previously, Mn1 ion is coordinated by six oxygen atoms from the carboxylate groups of BPTC ligands, but Mn2 is coordinated by only three oxygen atoms from the carboxylate groups and three coordinated solvent molecules in the SBU of **1** (Figure 3). After analyzing the coordination geometry of Mn2, we found that the three solvent molecules were located at the positions that every two solvent molecules are almost vertical. Hence, it is possible that every two coordinated solvent molecules can be replaced by

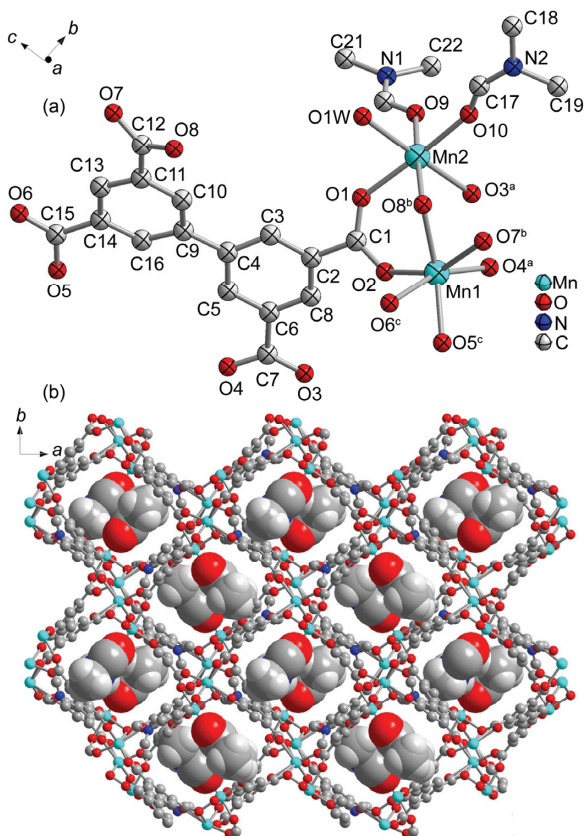


Figure 1 The asymmetric unit in **1** (a) uncoordinated DMF and water molecules are omitted for clarity and the 3D packing of **1** (b), showing the 1D channels along [001] direction, in which coordinated DMF reside. Symmetry codes: ^a $-x, 0.5+y, -0.5-z$; ^b $1-x, -1-y, -z$; ^c $x, -1.5-y, -0.5+z$.

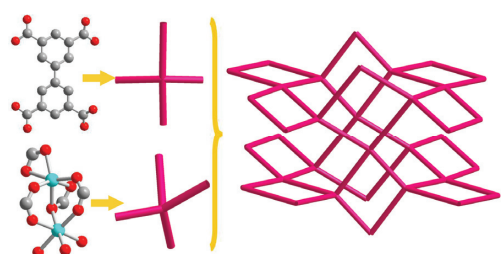


Figure 2 The PtS topology of complex **1** after simplifying the BPTC ligand as a planar node and the SBU as a tetrahedral node.

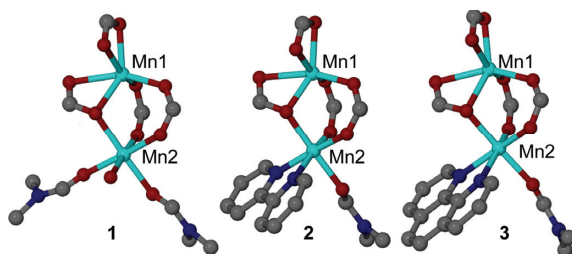


Figure 3 Coordination environment of Mn(II) centers in complexes **1–3**.

other chelating ligands such as bipy and phen without changing the geometry of the SBU as well as the framework.

Considering these, the solvothermal reactions of $\text{Mn}(\text{NO}_3)_2$, H_4BPTC , and bipy or phen were carried out. Fortunately, two new manganese coordination polymers, $\text{Mn}_2(\text{BPTC})(\text{bipy})(\text{DMF}) \cdot \text{DMF} \cdot \text{H}_2\text{O}$ (**2**), and $\text{Mn}_2(\text{BPTC})(\text{phen})(\text{DMF}) \cdot \text{EtOH}$ (**3**), were obtained with the same topology as **1**. Compared with complex **1**, complexes **2** and **3** were synthesized by changing the coordinated DMF and water molecules with chelating bipy or phen ligands (Figure 4), but the whole framework including the SBU and topology remains unchanged, and the coordination environment of Mn1 also keeps no change in the SBUs of **2** and **3**. However, Mn2 is coordinated by three oxygen atoms from the BPTC ligands, two nitrogen atoms from bipy or phen, and one oxygen atom from the coordinated DMF molecule. The average Mn–N distances are 2.121 (5) and 2.267 (4) Å for **2** and **3**, respectively. The average Mn–O distances in complexes **2** and **3** are 2.136 and 2.183 Å, respectively, which are shorter than that in complex **1**. Both **2** and **3** possess 1D channels along [001] direction, in which the coordinated bipy or phen molecules reside (Figure 5). The approximate channel sizes for compounds **2** and **3** are 5.3×9.0 and $4.3 \times 9.1 \text{ \AA}^2$, respectively. The percent void volume obtained using the PLATON software is 26.5% and 22.3% in the 3D networks of **2** and **3**.

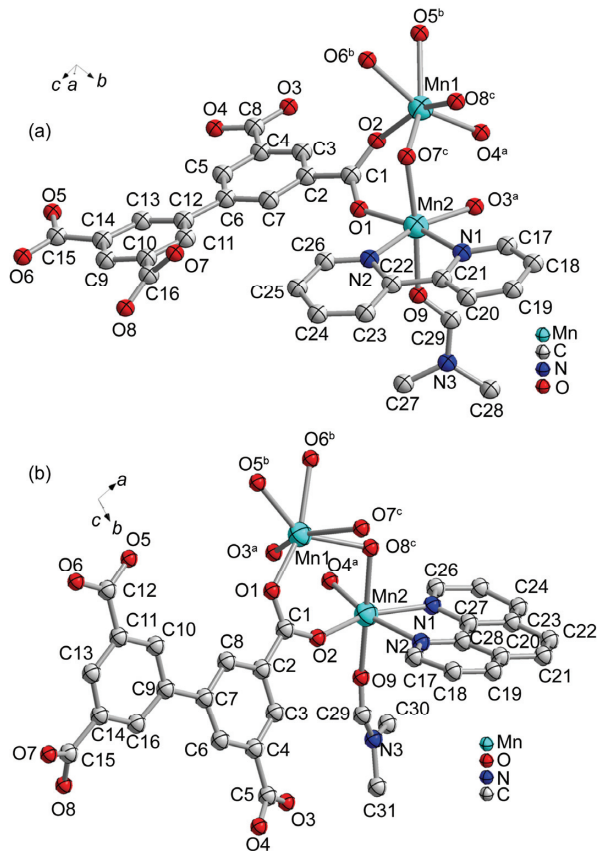


Figure 4 The coordination environment of **2** (a) (Symmetry codes: ^a $1-x, -0.5+y, -0.5-z$; ^b $1-x, -1-y, -1-z$; ^c $1+x, -0.5-y, -0.5+z$) and the coordination environment of **3** (b) uncoordinated DMF molecules are omitted for clarity (Symmetry codes: ^a $2.5-x, 0.5+y, -0.5-z$; ^b $-0.5+x, -0.5-y, -0.5+z$; ^c $2-x, -y, -1-z$).

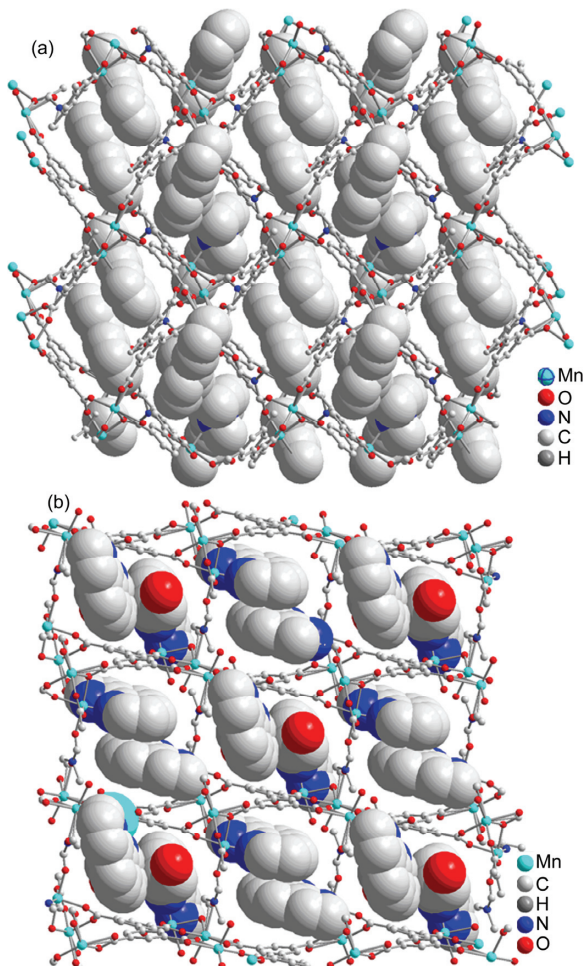


Figure 5 The 3D packing of complexes **2** (a) and **3** (b), showing the 1D channels along the [001] direction, with bipy and DMF residing in **2**, and phen and methanol in **3**.

TG analysis of **1** was performed in an N_2 atmosphere on polycrystalline sample, and the TG curve is shown in Figure 6. Complex **1** can be stable up to 150 °C where the coordinated DMF starts to decompose. The low thermal stability of **1** may derive from the being of three coordinated solvent molecules on one of the manganese ions in the SBU. The coordinated solvates are easy to be thermally released to result in the formation of unstable low-coordinated metal ions and further cause the collapsing of the whole framework. Therefore, replacing the coordinated solvent molecules by other chelating ligands such as 2,2'-bipyridine (bipy) and 1,10-phenanthroline (phen) becomes a facile strategy to improve the stability of the framework. Indeed, complex **2** is stable up to 400 °C where the coordinated bipy starts to decompose, whereas complex **3** is stable till 450 °C where the coordinated phen ligand begins to decompose according to TG analysis (Figure 6).

3.2 Magnetic properties

The variable-temperature magnetic measurement of complex

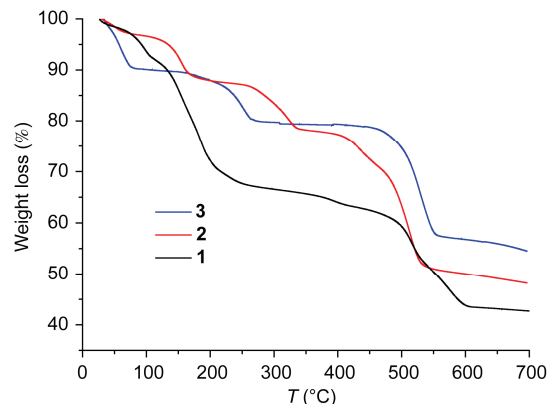


Figure 6 The TGA of the three complexes.

2 was performed in the temperature range of 1.8–300 K under an applied magnetic field of 1 kOe. The plots of $\chi_M T$ versus T together with $1/\chi_M$ versus T , where χ_M is the molar magnetic susceptibility per Mn_2 unit, are shown in Figure 7. The experimental $\chi_M T$ value of **2** at room temperature is 8.03 K cm³/mol, which is somewhat lower than the expected value of $\chi_M T = 8.75$ K cm³/mol for two independent high-spin Mn(II) centers with $g = 2.0$. The $\chi_M T$ product of **2** decreases slowly from ambient temperature to 75 K, and then reduces sharply to 0.16 K cm³/mol at 1.8 K, indicating an overall anti-ferromagnetic behavior. The magnetic susceptibility obeys the Curie-Weiss law down to 50 K with a Curie constant $C = 8.12$ K cm³/mol ($1/\chi_M = (T - \Theta)/C$) and a Weiss constant $\Theta = -3.28$ K.

3.3 Effect of the chelated ligand on the thermal stability of the final structures

It is well known that almost all of the applications of MOFs are highly determined by the framework stability. In the reported structures, the results demonstrated that some of the coordination sites of the metal ions are occupied by coordinated solvates such as H_2O and DMF, resulting in the formation of unstable low-coordination metal ions and further causing the collapse of the whole framework as the

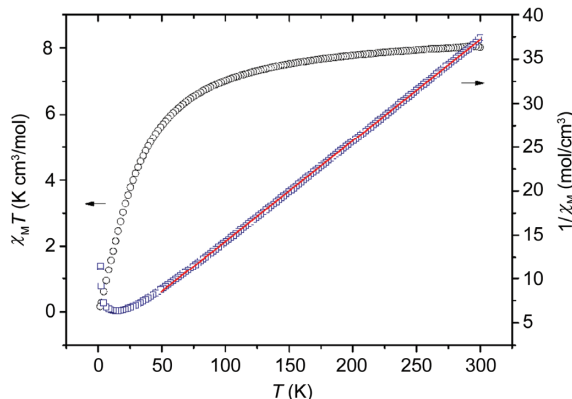


Figure 7 The variable-temperature magnetic measurement of complex **2**.

coordinated small solvates are easy to be thermally removed from the metal ions. In **1**, Mn²⁺ is coordinated by three oxygen atoms from three carboxylate groups, two coordinated DMF molecules, and one coordinated water molecule, that is, half of the coordination sites of Mn²⁺ ion are occupied by the solvent molecules. When the coordinated solvent molecules are thermally removed, the Mn²⁺ ion is only three-coordinate, which is extremely unstable. In fact, TG analysis displays that complex **1** is easy to lose coordinated solvent molecules at a low temperature, and bear low stability of framework. However, there is only one coordinated solvent molecule on the Mn²⁺ ion after replacing two coordinated solvates by chelating ligands in complexes **2** and **3**, which evidently improves the thermal stabilities of the frameworks.

4 Conclusions

In summary, we have synthesized a series of manganese-organic frameworks with PtS topology. The same topological MOFs can be successfully assembled without changing the geometries of the SBUs as well as the whole frameworks when substituting of two coordinated solvent molecules to chelating ligands, but the thermal stabilities of the MOFs are significantly improved.

This work was supported by the National Natural Science Foundation of China (21271117, 21201179), the Special Fund for Postdoctoral Innovation Program of the Shandong Province (201202040), the China Postdoctoral Science Foundation (2012M 510106), a project of the Shandong Province Higher Educational Science and Technology Program (J06A55), the Shandong Provincial Natural Science Foundation (ZR2010BL011), the Shandong Natural Science Fund for Distinguished Young Scholars (BS2012CL038), and the Fundamental Research Funds for the Central Universities (12CX04092A, 13CX05015A).

- 1 Yang GP, Hou L, Luan XJ, Wu B, Wang YY. Molecular braids in metal-organic frameworks. *Chem Soc Rev*, 2012, 41: 6992–7000
- 2 Kim M, Cahill JF, Fei HH, Prather KA, Cohen SM. Postsynthetic ligand and cation exchange in robust metal-organic frameworks. *J Am Chem Soc*, 2012, 134: 18082–18088
- 3 He YP, Tan YX, Zhang J. Stable Mg-metal-organic framework (MOF) and unstable Zn-MOF based on nanosized tris((4-carboxyl)phenylduryl)amine ligand. *Cryst Growth Des*, 2013, 13: 6–9
- 4 Yang QX, Chen XQ, Chen ZJ, Hao Y, Li YZ, Zheng HG. Metal-organic frameworks constructed from flexible V-shaped ligands: adjustment of the topology, interpenetration and porosity via a solvent system. *Chem Comm*, 2012, 48: 10016–10018
- 5 Stock N, Biswas S. Synthesis of metal-organic frameworks (MOFs): routes to various MOF topologies, morphologies, and composites. *Chem Rev*, 2012, 112: 933–969
- 6 Song YF, Cronin L. Postsynthetic covalent modification of metal-organic framework (MOF) materials. *Angew Chem Int Ed*, 2008, 47: 4635–4637
- 7 Tanabe KK, Wang Z, Cohen SM. Systematic functionalization of a metal-organic framework via a postsynthetic modification approach. *J Am Chem Soc*, 2008, 130: 8508–8517
- 8 Zhan WW, Kuang Q, Zhou JZ, Kong XJ, Xie ZX, Zheng LX. Semi-

conductor@metal-organic framework core-shell heterostructures: a case of ZnO@ZIF-8 nanorods with selective photoelectrochemical response. *J Am Chem Soc*, 2013, 135: 1926–1933

- 9 Walton KS, Millward AR, Dubbeldam D, Frost H, Low JJ, Yaghi OM, Snurr RQ. Understanding inflections and steps in carbon dioxide adsorption isotherms in metal-organic frameworks. *J Am Chem Soc*, 2008, 130: 406–407
- 10 Singh NK, Hardi M, Balema VP. Mechanochemical synthesis of an yttrium based metal-organic framework. *Chem Commun*, 2013, 49: 972–974
- 11 Vincent JM. Recent advances of fluorous chemistry in material sciences. *Chem Comm*, 2012, 48: 11382–11391
- 12 Jiang HL, Feng DW, Liu TF, Li JR, Zhou HC. Pore surface engineering with controlled loadings of functional groups via click chemistry in highly stable metal-organic frameworks. *J Am Chem Soc*, 2012, 134: 14690–14693
- 13 Li CP, Wu JM, Du M. Exceptional crystallization diversity and solid-state conversions of Cd^{II} coordination frameworks with 5-bromonicotinate directed by solvent media. *Chem A Eur J*, 2012, 18: 12437–12445
- 14 Zou C, Wu CD. Functional porphyrinic metal-organic frameworks: crystal engineering and applications. *Dalton Trans*, 2012, 41: 3879–3888
- 15 Kirillov AM. Hexamethylenetetramine: an old new building block for design of coordination polymers. *Coord Chem Rev*, 2011, 255: 1603–1622
- 16 Dhakshinamoorthy A, Garcia H. Catalysis by metal nanoparticles embedded on metal-organic frameworks. *Chem Soc Rev*, 2012, 41: 5262–5284
- 17 Paz FAA, Klinowski J, Viela SMF, Tome JPC, Cavaleiro JAS, Rocha J. Ligand design for functional metal-organic frameworks. *Chem Soc Rev*, 2012, 41: 1088–1110
- 18 Cohen SM. Modifying MOFs: new chemistry, new materials. *Chem Sci*, 2010, 1: 32–36
- 19 Qiu SL, Zhu GS. Molecular engineering for synthesizing novel structures of metal-organic frameworks with multifunctional properties. *Coord Chem Rev*, 2009, 293: 2891–2911
- 20 Jin CM, Zhu Z, Chen ZF, Hu YJ, Meng XG. An unusual three-dimensional water cluster in metal-organic frameworks based on ZnX₂ (X = ClO₄, BF₄) and an Azo-functional ligand. *Cryst Growth Des*, 2010, 10: 2054–2056
- 21 Zhang WH, Dong Z, Wang YY, Hou L, Jin JC, Huang WH, Shi QZ. Synthesis, structural diversity and fluorescent characterization of a series of d¹⁰ metal-organic frameworks (MOFs): reaction conditions, secondary ligand and metal effects. *Dalton Trans*, 2011, 40: 2509–2521
- 22 Zhao D, Timmons DJ, Yuan D, Zhou HC. Tuning the topology and functionality of metal-organic frameworks by ligand design. *Acc Chem Res*, 2010, 44: 123–133
- 23 Suhyun SH, Kim JY, Kim SJ, Park S. Two-dimensional metal-organic frameworks with blue luminescence *Dalton Trans*, 2010, 39: 1261–1265
- 24 Liu GX, Huang YQ, Chu Q, Okamura T, Sun WY, Liang H, Ueyama N. Effect of N-donor ancillary ligands on supramolecular architectures of a series of zinc(II) and cadmium(II) complexes with flexible tricarboxylate. *Cryst Growth Des*, 2008, 8: 3233–3245
- 25 Sun DF, Ke YX, Mattox TM, Betty AO, Zhou HC. Temperature-dependent supramolecular stereoisomerism in porous copper coordination networks based on a designed carboxylate ligand. *Chem Comm*, 2005, 43: 5447–5449
- 26 Humphrey SM, Chang JS, Jhung SH, Yoon JW, Wood PT. Porous cobalt(II)-organic frameworks with corrugated walls: structurally robust gas-sorption materials. *Angew Chem Int Ed*, 2007, 46: 272–275
- 27 Coronado E, Espallargas GM. Dynamic magnetic MOFs. *Chem Soc Rev*, 2013, 42: 1525–1539

- 28 Han ZB, Lu RY, Liang YF, Zhou YL, Chen Q, Zeng MH. Mn(II)-based porous metal-organic framework showing metamagnetic properties and high hydrogen adsorption at low pressure. *Inorg Chem*, 2012, 51: 674–679
- 29 Panda T, Pachfule P, Banerjee R. Template induced structural isomerism and enhancement of porosity in manganese(II) based metal-organic frameworks (Mn-MOFs). *Chem Comm*, 2011, 47: 7674–7676
- 30 Liu XF, Oh M, Myoung S. size- and shape-selective isostructural microporous metal-organic frameworks with different effective aperture sizes. *Inorg Chem*, 2011, 50: 5044–5053
- 31 Prakash MJ, Lah MS. Metal-organic macrocycles, metal-organic polyhedra and metal-organic frameworks. *Chem Comm*, 2009, 23: 3326–3341
- 32 Li JR, Kuppler RJ, Zhou HC. Selective gas adsorption and separation in metal-organic frameworks. *Chem Soc Rev*, 2009, 38: 1477–1504
- 33 Wang XS, Ma SQ, Zhou HC. Metal-organic frameworks based on double-bond-coupled di-isophthalate linkers with high hydrogen and methane uptakes. *Chem Mater*, 2008, 20: 3145–3152
- 34 Ma LQ, Lin WB. Unusual interlocking and interpenetration lead to highly porous and robust metal-organic frameworks. *Angew Chem Int Ed*, 2009, 48: 3637–3640
- 35 Wu ST, Ma LQ, Long LS, Zheng LS, Lin WB. Three-dimensional metal-organic frameworks based on functionalized tetracarboxylate linkers: synthesis, structures, and gas sorption studies. *Inorg Chem*, 2009, 48: 2436–2442
- 36 Liu CS, Sañudo EC, Hu M, Zhou LM, Guo LQ, Ma ST, Gao LJ, Fang SM. Metal-organic coordination polymers based on a flexible tetrahydrofuran-2,3,4,5-tetracarboxylate ligand: syntheses, crystal structures, and magnetic/photoluminescent properties. *CryEngComm*, 2010, 12: 853–865
- 37 Yang GS, Lan YQ, Zang HY, Shao KZ, Wang XL, Su ZM, Jiang CJ. Two eight-connected self-penetrating porous metal-organic frameworks: configurational isomers caused by different linking modes between terephthalate and binuclear nickel building units. *CryEngComm*, 2009, 11: 274–277
- 38 He HY, Collins D, Dai FN, Zhao XL, Zhang GQ, Ma HQ, Sun DF. Construction of metal-organic frameworks with 1D chain, 2D grid, and 3D porous framework based on a flexible imidazole ligand and rigid benzenedicarboxylates. *Crystal Growth Des*, 2010, 10: 895–902
- 39 Liu HY, Wu H, Yang J, Liu YY, Liu B, Liu YY, Ma JF. pH-dependent assembly of 1D to 3D octamolybdate hybrid materials based on a new flexible bis-[(pyridyl)-benzimidazole] ligand. *Crystal Growth Des*, 2011, 11: 2920–2927
- 40 Li QW, Zhang WY, Miljanic OS, Sue CH, Zhao YL, Liu LH, Knobler CB, Stoddart JF, Yaghi OM. Docking in metal-organic frameworks. *Science*, 2009, 325: 855–859
- 41 Wang HL, Zhang DP, Sun DF, Chen YT, Zhang LF, Tian LJ, Jiang JZ. Co(II) metal-organic frameworks (MOFs) assembled from asymmetric semirigid multicarboxylate ligands: synthesis, crystal structures, and magnetic properties. *Crystal Growth Des*, 2009, 12: 5273–5282
- 42 Kan WQ, Liu YY, Yang J, Liu YY, Ma JF. Syntheses, structures and photoluminescent properties of a series of metal-organic frameworks based on a flexible tetracarboxylic acid and different bis(imidazole) ligands. *CryEngComm*, 2011, 13: 4256–4269
- 43 O'Keeffe M, Eddaoudi M, Li HL, Reineke T, Yaghi OM. Frameworks for extended solids: geometrical design principles. *J Solid State Chem*, 2000, 152: 3–20
- 44 Chen BL, Eddaoudi M, Reineke TM, Kampf JW, O'keeffe M, Yaghi OM. Cu₂(ATC) · 6H₂O: design of open metal sites in porous metal-organic crystals (ATC:1,3,5,7-adamantane tetracarboxylate). *J Am Chem Soc*, 2000, 122: 11559–11560
- 45 Nattinen KI, Rissanen K. Ligand entrapment in twofold interpenetrating PtS matrixes by metallo-organic frameworks. *Inorg Chem*, 2003, 42: 5126–5134
- 46 Zhang J, Xue YS, Liang LL, Ren SB, Li YZ, Du HB, You XZ. Porous coordination polymers of transition metal sulfides with PtS topology built on a semirigid tetrahedral linker. *Inorg Chem*, 2010, 49: 7685–7691
- 47 Zheng B, Luo JH, Wang F, Peng Y, Li GH, Huo QS, Liu YL. Construction of six coordination polymers based on a 5,5'-(1,2-ethynyl)bis-1,3-benzenedicarboxylic ligand: synthesis, structure, gas sorption, and magnetic properties. *Cryst Grow Des*, 2013, 13: 1033–1044
- 48 Czaia AU, Trukhan N, Mueller U. Industrial applications of metal-organic frameworks. *Chem Soc Rev*, 2009, 38: 1284–1293
- 49 Pan L, Parker B, Huang XY, Olson DH, Lee J, Li J. Zn(tbip) (H₂tbip = 5-*tert*-butyl isophthalic acid): a highly stable guest-free microporous metal organic framework with unique gas separation capability. *J Am Chem Soc*, 2006, 128: 4180–4181
- 50 Chen XY, Zhao B, Shi W, Xia J, Cheng P, Liao DZ, Yan SP, Jiang ZH. Microporous metal-organic frameworks built on a Ln₃ cluster as a six-connecting node. *Chem Mater*, 2005, 17: 2866–2874
- 51 Black CA, Costa J, Fu WT, Massera C, Roubeau O, Teat SJ, Aromi G, Gamez P, Reedijk J. 3D lanthanide metal-organic frameworks: structure, photoluminescence, and magnetism. *Inorg Chem*, 2009, 48: 1062–1068
- 52 Huang W, Wu D, Zhou P, Yan WB, Guo D, Duan CY, Meng QJ. Luminescent and magnetic properties of lanthanide-thiophene-2,5-dicarboxylate hybrid materials. *Cryst Growth Des*, 2009, 9: 1361–1369
- 53 Zhao XJ, Zhu GS, Fang QR, Wang Y, Sun FX, Qiu SL. A series of three-dimensional lanthanide coordination compounds with the rutile topology. *Cryst Growth Des*, 2009, 9: 737–742
- 54 Sheldrick GM. SHELXS-97, program for crystal structure solution. Göttingen: Göttingen University, 1997
- 55 Sheldrick GM. SHELXL-97, program for crystal structure refinement. Göttingen: Göttingen University, 1997